ICAS 2020 SHANG HAI
International Council of the Aeronautical Sciences
32nd Congress of the International Council of the Aeronautical Sciences
September 6-10, 2021
Pudong Shangri-La, Shanghai, China

HELICOPTER ROTOR AERODYNAMIC PERFORMANCE PREDICTION BASED ON FLOW SIMULATION AROUND AIRFOILS

S-Z. Zhao*, X. Zhao*, K. You*, M-H. Kang*, Y-F. Lin**

*National Key Laboratory of Science and Technology on Aerodynamic Design and Research, Northwestern Polytechnical University, Xi'an, Shaanxi, 710072, China
**China Helicopter Research and Development Institute, Jingdezhen, Jiangxi, 333001,China

Abstract

With the increase of flight speed, helicopter rotor aerodynamic environment becomes complicated. Transonic flow near the forward blade tip and reverse flow near the backward blade root occured at the same time. In order to estimate rotor aerodynamic performance, the CFD simulation around airfoils on various working conditions were carried out. First, transient flow simulations around NACA0012 airfoil were tested for various turbulence models at several working conditions (Ma number 0.28~0.8, angle of attack 10~20°, 160~180°). Results were compared with experimental values. It was found that the Realizable k-epsilon turbulence model was closer to the test than kkl omega turbulent model. The errors of the lift coefficient and drag coefficient were -46.7~56.3% and -66.2~27.5% respectively. Secondly, airfoils on the XH-59A helicopter rotor (NACA0026, NACA63-213, NACA63-218, NACA63-224 and NACA230125) were simulated in various working conditions. Finally, with the airfoil performance database provided, the rotor performance in advance ratio 0.1~0.4 was obtained based on momentum blade element theory.

Keywords: aerodynamic performance, flow simulation around airfoils

1. Introduction

When a helicopter flies at a high advance ratio, the flow phenomenon is complicated, and the rotor will be affected by the reverse flow, see Figure 1. The higher the forward flight speed, the larger the reverse flow region and the more serious the stall problem. Therefore, the separation of airflow also limits the forward flight speed of the helicopter.

Generally, flow across the airfoil from the leading edge to the trailing edge can be named as downstream. Instead, it across the trailing edge to the leading edge is named as reverse flow. In this situation, the flow at leading and trailing edges of the airfoil are more likely to separate, resulting in reduction of maximum lift, the resistance divergence angle of attack, and the increment of the stall angle of attack. The pitch moment changes sharply near the 0° angle of attack, and the aerodynamic characteristics are obviously inferior to downstream conditions.

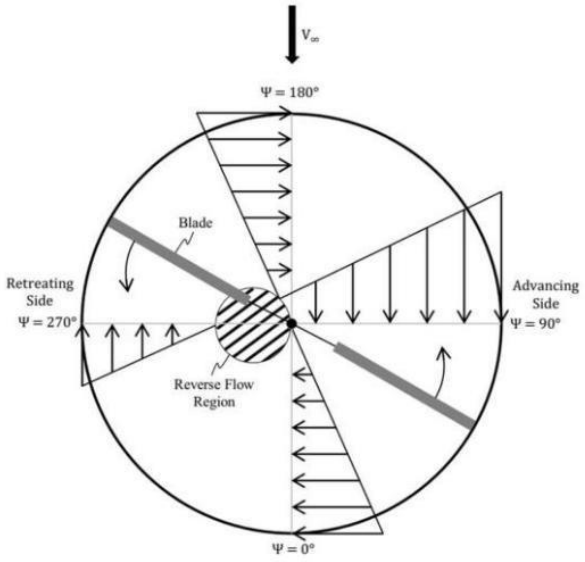

Figure 1. Reverse flow region.

Research on the reverse flow is quite limited. There is short of experimental data and simulation is inadequate. Ai [1] used the SA model in the Reynolds Average Model (RANS) and the SA-DDES model in the LES to calculate the flow field around the delta wing under multiple conditions, and verified that the SA-DDES was more accurate than the SA model. Zhou [2] proved that DES could better simulate the large-scale separation flow around a two-dimensional airfoil than the RANS method, and could simulate the flow field more detailed. However, in addition to the slight deviation of the calculation results of certain azimuth angles when the flow was separated, the results in other cases were basically the same. Therefore, the RANS method was adopted in this paper to save time and resources.

Kong and Chen [3] took the H-34 rotor as an example. The influence of the reverse flow region on the rotor aerodynamic characteristics was calculated and analyzed under high advance ratio, and compared with wind tunnel test data.

It can be seen that the performance of the airfoil in the reverse flow region is greatly affected by the selected turbulence model. It is necessary to select a suitable turbulence model through the CFD method to obtain more accurate aerodynamic performance.

2. NACA0012 Airfoil Performance Simulation and Validation

The NACA0012 airfoil wind tunnel test data [4] was applied for CFD model. ANSYS ICEM software was employed to create the mesh. In order to ensure the accuracy of calculation, when constructing the NACA0012 airfoil model, the trailing edge of the airfoil was filleted first, the purpose was to calculate that the trailing edge was not prone to flow separation during the reverse flow. Yuan [5] verified the beneficial effect of the trailing edge rounding on the reverse flow characteristics. The model of NACA0012 airfoil fillet is shown in **Figure 2**.

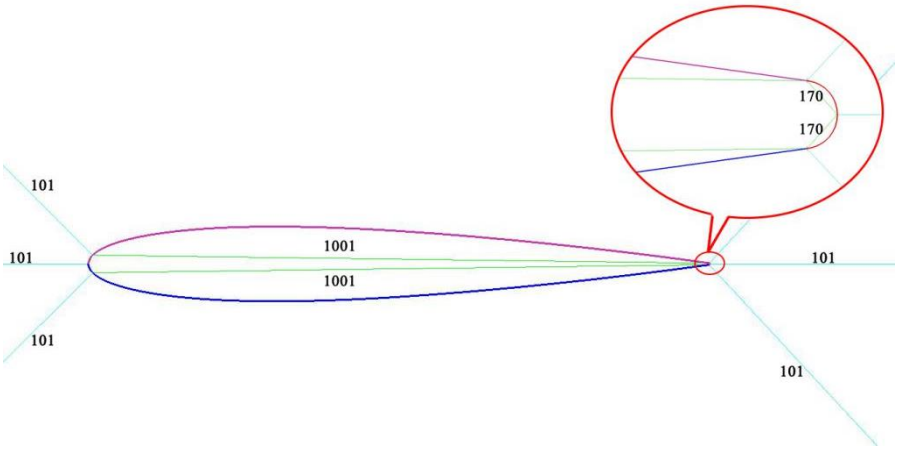

Figure 2. The fillet of the trailing edge of the NACA0012 airfoil.

The original airfoil chord length was 0.1m, with far field radius 20 times of the chord length. It would be scaled according to the chord length in various working conditions in **Table 1**. The grids division the leading edge and trailing edge of the airfoil, along chord direction and in radial direction were 340, 1000 and 101 respectively. The first boundary layer grid thickness of the airfoil was the 10^{-5} times of the chord length. The total number of grids was 2.7×10^{5}. The local meshes of the leading and trailing edges of the NACA0012 airfoil are shown in **Figure 3**.

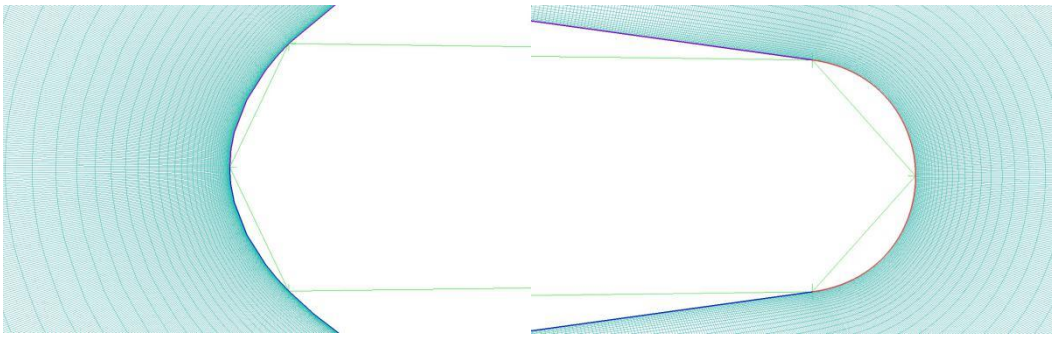

Figure 3. Local meshes of the leading and trailing edges of the NACA0012 airfoil.

The wind tunnel experiment provided lift-drag coefficient or pressure coefficient of NACA0012 airfoil under 5 working conditions. The representative data was selected for verification with corresponding working conditions shown in **Table 1**.

Table 1. NACA0012 airfoil working conditions and performance

Ma	0.28	0.3	0.8	0.82	0.82
Re	3.47×10^{6}	3.72×10^{6}	9.92×10^{6}	10.17×10^{6}	3×10^{6}
Chord length(m)	0.53297	0.53297	0.53287	0.53297	0.10625
Angle of attack(°)	10~30, 160~180	10~25, 145~175	10~25, 145~175	10~30, 160~180	-0.14
Coefficient	C_d	C_l	C_l	C_d	C_p

Transient airflow models were developed by software FLUENT. K-kl-omega and Realizable k-epsilon turbulent models were compared, Turbulence viscosity ratio was set to 4. Density-based solution was applied and pressure far-field boundary condition were adopted. The unsteady equation was solved by a first-order implicit scheme, and flow was solved by a second-order upwind scheme. The time step was chosen as 1×10^{-4} s, and the number of internal iterations was set to 50.

The airfoil lift and drag coefficients at angles of attack of 10-20° (downstream) and 145-175° (reverse flow) were calculated. Results are compared with experimental data in **Figure 4** and **Figure 5**. Detailed data are shown in **Table 2**.

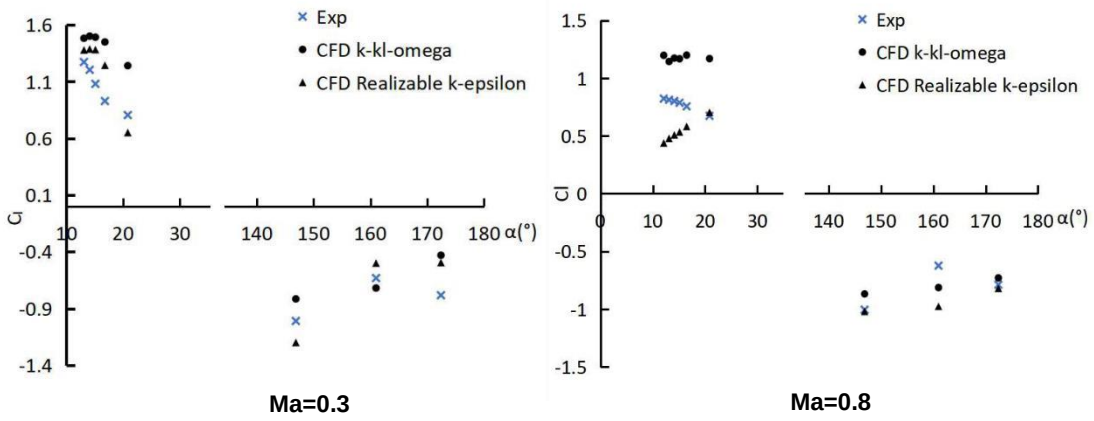

Figure 4. NACA0012 airfoil lift coefficient varies with the angle of attack.

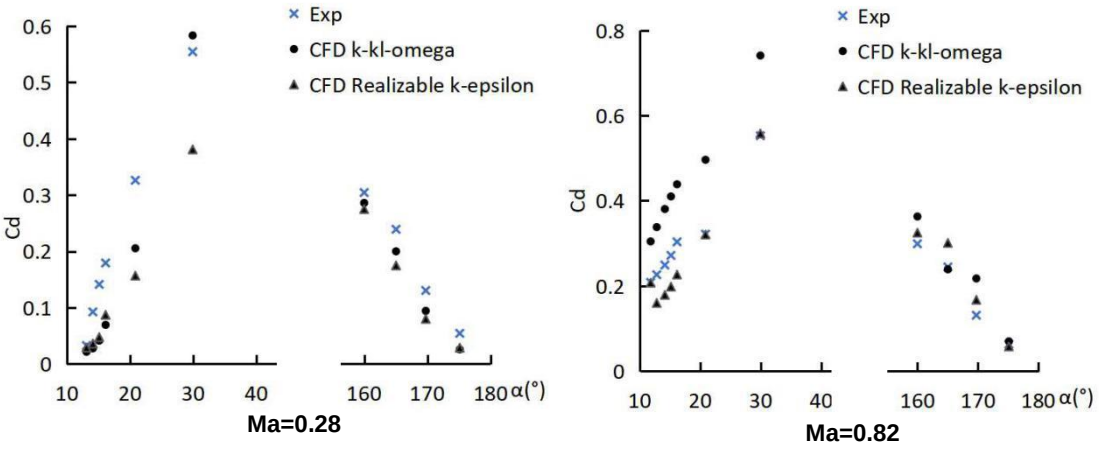

Figure 5. NACA0012 airfoil drag coefficient varies with angle of attack.

The **Table 2** also gives the relative error of each numerical calculation result based on the experimental value. According to **Formula (1)**, the standard deviation of the numerical results was solved for the four sets of Ma number working conditions.

$$\sigma = \sqrt{\frac{1}{N}\sum_{i=1}^{N}(X_{i(CFD)} - X_{i(EXP)})^2} \qquad (1)$$

For simplicity, the experimental value is abbreviated as Exp, k-kl-omega is abbreviated as KKO, and Realizable k-epsilon is abbreviated as RKE.

Figures 4 ~ **5** and **Table 2** show that in the calculation of lift coefficient, the Realizable k-epsilon calculation result in the downstream region is closer to the experimental value. The error range is -19.2~34% (0.3Ma) and -46.7~4.5% (0.8Ma), the standard deviation is 0.228 (0.3Ma) and 0.271 (0.8Ma). The error range of k-kl-omega is 16.5~56.1% (0.3Ma) and 40.8~73.6% (0.8Ma), with standard deviations of 0.39 (0.3Ma) and 0.425 (0.8Ma). The calculation results of the two models in the reverse flow region are not much different.

Table 2. Aerodynamic performance results comparison of NACA0012 airfoil

Angle (°)	Ma=0.3			Ma=0.8			Ma=0.28			Ma=0.82		
	C_l /relative error %						C_d /relative error %					
	Exp	KKO	RKE	Exp	KKO	RKE	Exp	KKO	RKE	Exp	KKO	RKE
12	/	/	/	0.822	1.196 /45.5	0.438 /-46.7	/	/	/	0.208	0.304 /46.2	0.208 /-0.4
13	1.271	1.481 /16.5	1.378 /8.4	0.817	1.243 /53.1	0.478 /-41.1	0.033	0.022 /-33.6	0.029 /-10.5	0.226	0.338 /49.3	0.160 /-29.3
14	1.203	1.500 /24.7	1.387 /15.3	0.801	1.272 /58.7	0.508 /-36.6	0.092	0.028 /-70.0	0.036 /-60.8	0.249	0.381 /52.8	0.179 /-28.1
15	1.079	1.490 /38.1	1.381 /28.0	0.786	1.292 /64.4	0.533 /-32.2	0.141	0.041 /-70.7	0.048 /-66.2	0.272	0.410 /50.9	0.198 /-27.0
16	/	/	/	0.755	1.198 /58.6	0.582 /-23.0	0.179	0.069 /-61.3	0.087 /-51.4	0.303	0.439 /44.5	0.227 /-25.3
17	0.928	1.448 /56.1	1.244 /34.0	/	/	/	/	/	/	/	/	/
21	0.804	1.240 /54.2	0.650 /-19.2	0.673	1.168 /73.6	0.703 /4.5	0.326	0.205 /-37.0	0.157 /-51.9	0.322	0.496 /54.6	0.321 /-0.3
σ	/	0.390	0.228	/	0.425	0.271	/	0.083	0.115	/	0.143	0.054
147	-1.010	-0.816 /-19.2	-1.200 /18.8	-1.005	-0.868 /-13.6	-1.020 /1.5	/	/	/	/	/	/
160	/	/	/	/	/	/	0.304	0.286 /-6.0	0.275 /-9.6	0.299	0.363 /21.4	0.325 /8.7
161	-0.632	-0.720 /13.9	-0.500 /-20.9	-0.634	-0.813 /30.3	-0.975 /56.3	/	/	/	/	/	/
165	/	/	/	/	/	/	0.239	0.200 /-16.4	0.175 /-26.8	0.245	0.239 /-2.3	0.301 /23.1
170	/	/	/	/	/	/	0.130	0.094 /-27.7	0.080 /-38.7	0.131	0.218 /65.7	0.168 /27.5
172	-0.784	-0.431 /-45.0	-0.496 /-36.8	-0.789	-0.730 /-7.5	-0.820 /4.0	/	/	/	/	/	/
175	/	/	/	/	/	/	0.054	0.026 /-52.3	0.029 /-47.1	0.063	0.070 /10.2	0.058 /-8.5
σ	/	0.238	0.213	/	0.139	0.176	/	0.032	0.045	/	0.054	0.036

In the calculation of the drag coefficient, the calculation results of the two turbulence models at 0.28Ma in the downstream region are not much different. However, the calculation accuracy of Realizable k-epsilon at 0.82Ma is significantly higher than that of the k-kl-omega model, with standard deviations of 0.054 and 0.143, respectively. In addition, the calculation errors of the two models under the two working conditions of the reverse flow region are similar. It is concluded from the above analysis that the Realizable k-epsilon model is more accurate.

Due to the consideration of airfoil transonic flow characteristics, local flow details are needed to verify the

experimental results. Therefore, it is necessary to verify the accuracy of the Realizable k-epsilon model in the airfoil pressure coefficient, and compare with the experimental data in literature [6]. In the experiment, the airfoil Mach number was 0.82, the Reynolds number was 3×10^6, the angle of attack was -0.14° , and the airfoil chord length was 106.25mm. Density base and unsteady settings were used for calculation in FLUENT. The result comparison is shown in **Figure 6**.

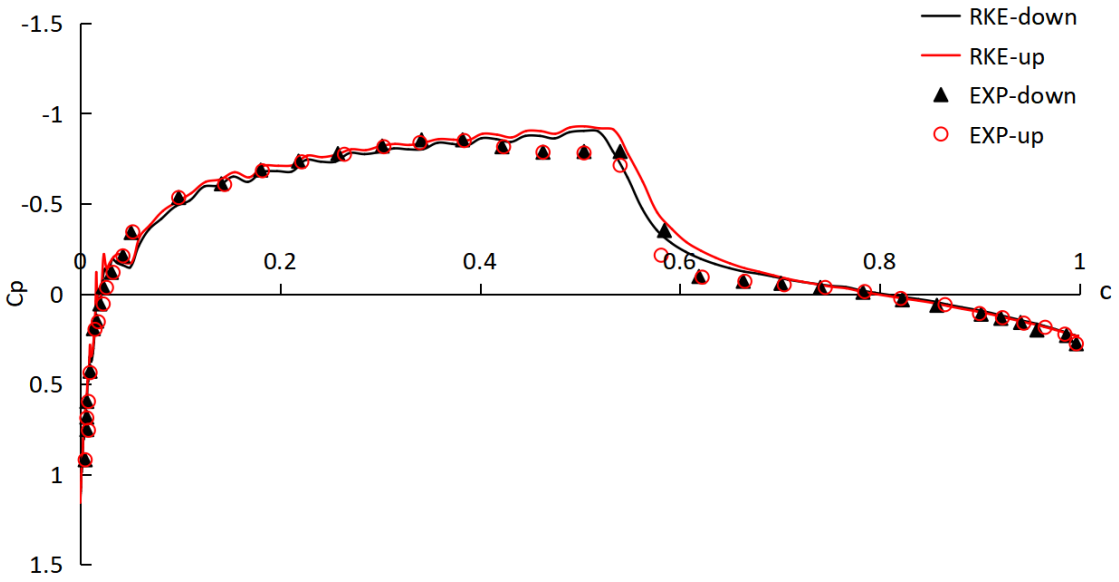

Figure 6. Pressure coefficient varies with chord length of the NACA0012 airfoil.
(Ma=0.82， Re=3×10^6，α=-0.14°)

Figure 6 shows that the airfoil pressure coefficient predicted by CFD is basically consistent with the experimental value, and the shock wave generation position is slightly earlier. The shock wave positions of the upper and lower wings obtained by CFD are 50.7%c and 51%c, and the experimental shock wave positions are 54%c and 54%c. The peak pressure coefficient is basically the same, with an error of 5.48%.

The comparison of various data proves that the Realizable k-epsilon turbulence model has high accuracy and reliability in calculating the aerodynamic characteristics of the airfoil. Therefore, when predicting the airfoil of each section of the XH-59A rotor, choose to use Realizable k-epsilon turbulence model for calculation.

3. Airfoils of XH-59A Helicopter Rotor Performance Simulation

The appearance of the XH-59A helicopter rotor is shown in **Figure 7**. The rotor radius was 5.49m with blade torsion angle -10°. The 0.105 section adopted NACA0026 airfoil with a chord length of 0.16m. The 0.2 section adopted NACA63(230)-224A airfoil with a chord length of 0.5m. The 0.43 section adopted NACA63(230)-218A airfoil with a chord length of 0.45m. The 0.625 section adopted NACA63(230)-213A airfoil with a chord length of 0.39m. NACA23012 (64) airfoil was used from the 0.725 section to the blade tip, and the chord length was 0.37m and 0.28m respectively.

Because the modified airfoil shape was not available, the uncorrected airfoil was used instead (NACA0026, NACA63-213, NACA63-218, NACA63-224, NACA23012). The same method was used for the numerical simulation of 5 airfoils of 6 sections of XH-59A. The airfoil geometry model was also optimized with the fillet of the trailing edge, and the mesh was divided using the same parameters as the NACA0012 airfoil verification. The total number of grids was 2.7×10^5.

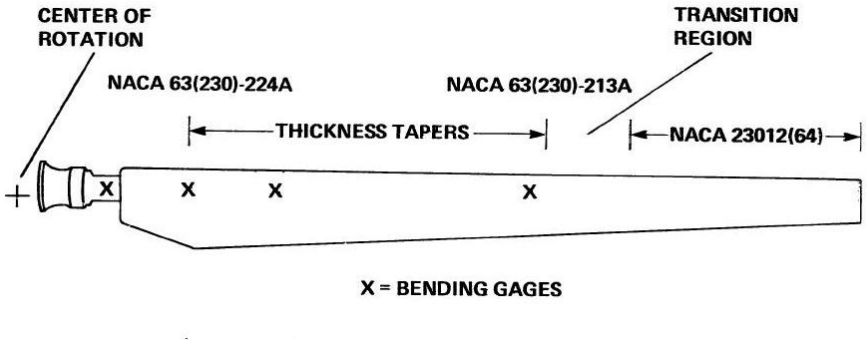

Figure 7. Sketch of the rotor blade.

In order to simulate rotor aerodynamic force, the chord length of each section airfoil were selected according to the actual rotor. Four Mach number conditions of 0.2, 0.4, 0.6, 0.8 were chosen. There were 17 angles of attack within the range of 0~20° and 160~180° , which constituted a total of 408 working conditions. The working conditions parameters is shown in **Table 3**.

Table 3. Mach number and Reynolds number for airfoil calculation conditions(Ma, Re in 10^6)

Airfoil of different sections / Actual chord length(m)											
NACA 0026 /0.16329		NACA 63224 /0.50292		NACA 63218 /0.45067		NACA 63213 /0.39188		NACA 23012 /0.36576		NACA 23012 /0.27759	
0.2	0.745	0.2	2.296	0.2	2.057	0.2	1.789	0.2	1.67	0.2	1.267
0.4	1.491	0.4	4.591	0.4	4.114	0.4	3.578	0.4	3.339	0.4	2.534
0.6	2.236	0.6	6.887	0.6	6.171	0.6	5.366	0.6	5.009	0.6	3.801
0.8	2.981	0.8	9.183	0.8	8.229	0.8	7.155	0.8	6.678	0.8	5.068

All working conditions of XH-59A were calculated using the batch processing method of FLUENT, and the unsteady calculation method was used. Similar solver setting were accepted with NACA0012 airfoils.

Take the working condition of forward ratio μ=0.3 as an example, the aerodynamic force prediction of XH-59A rotor airfoils are shown in **Figures 8~9**.

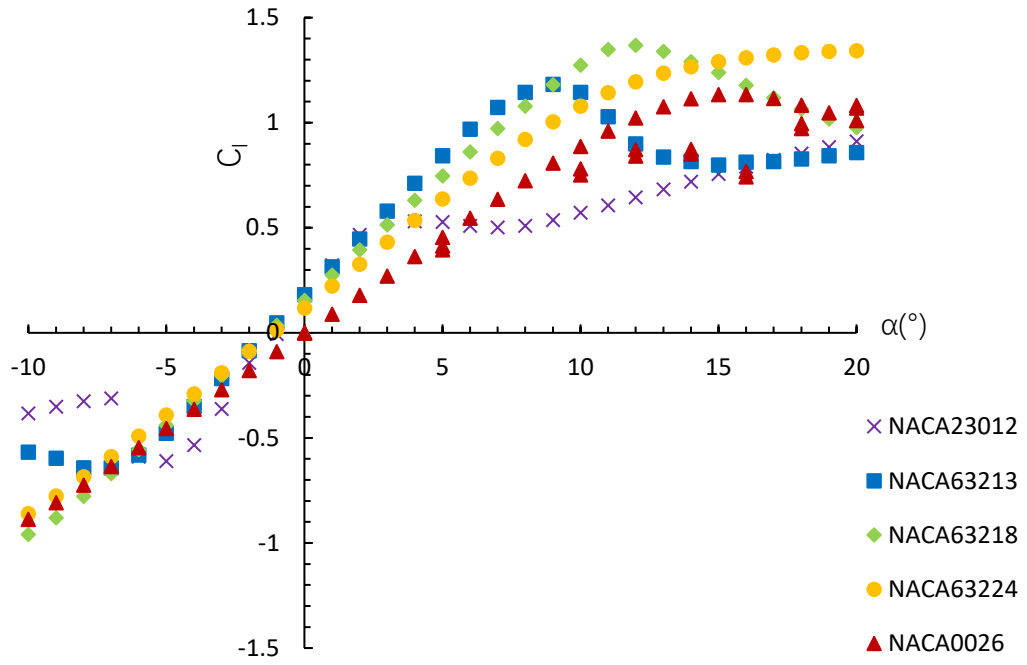

Figure 8. Summary of the XH-59A rotor blade airfoils lift coefficients.

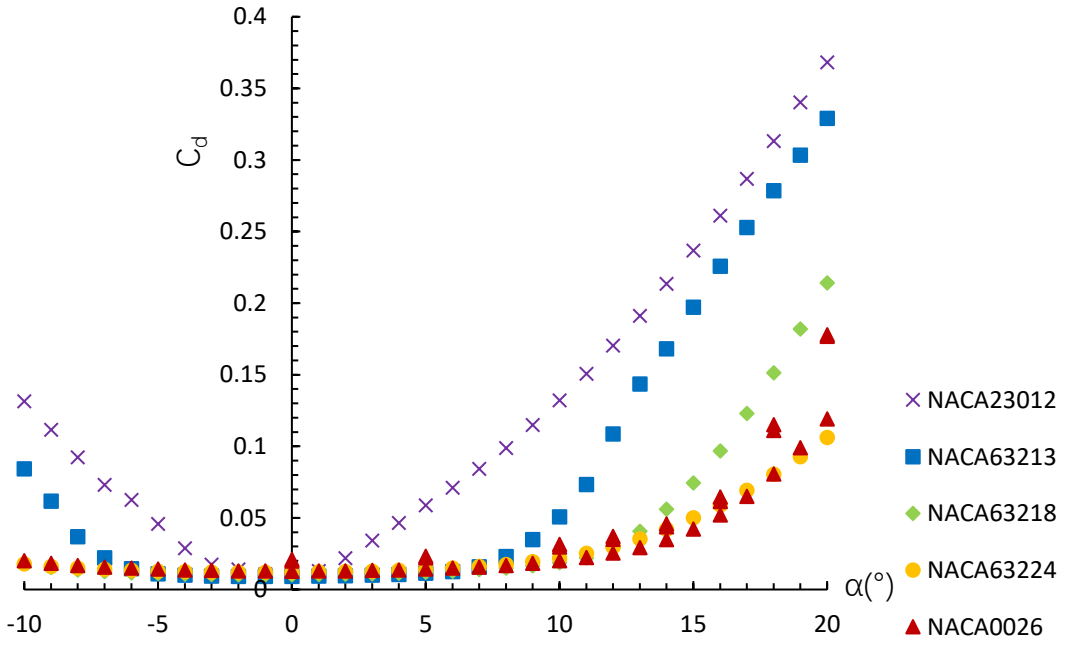

Figure 9. Summary of the XH-59A rotor blade airfoils drag coefficients.

The results were used to form a database for rotor thrust and torque prediction in helicopter forward flight.

4. Rotor Aerodynamic Performance Prediction

With the airfoil database generated, the neural network method was used to compile the MATLAB program to obtain the airfoil aerodynamic characteristics under other conditions by interpolation. Then the momentum blade element theory of the rotor in forward flight was developed to calculate the XH-59A rotor thrust, torque and power, under the working conditions of 0.1~0.4 advance ratio. This work will be present later on.

5. Conclusion

Unsteady flow across the airfoils were carried out on NACA0012 airfoils under 5 working conditions using the Realizable k-epsilon and k-kl-omega turbulence models. Results were validated with experimental data.

Simulation results show that Realizable k-epsilon model is more accurate than k-kl-omega turbulence models referring to experimental value. (I) For lift coefficient, in the downstream flow region, the former is more accurate. The error range is -19.2~34% (0.3Ma) and -46.7~4.5% (0.8Ma), the standard deviation is 0.228 (0.3Ma) and 0.271 (0.8Ma). In the reverse flow region, the calculation results of the two models are not much different. (ii) For drag coefficient, in the downstream region, the calculation accuracy of Realizable k-epsilon at 0.82Ma is significantly higher than that of the k-kl-omega model, with standard deviations of 0.054 and 0.143, respectively. The calculation results of the two turbulence models at 0.28Ma are not much different. In the reverse flow, the calculation errors of the two models under the two working conditions are similar. (iii) The airfoil pressure coefficient predicted by realizable k-epsilon is basically consistent with the experimental value, and the shock wave generation position is slightly earlier.

Based on realizable k-epsilon model, the unsteady flow simulations around five airfoils on XH-59A rotor were carried out. Altogether 12 working conditions were completed with flow range in 0.2Ma~0.8Ma and attack angle -10~20° and 160~190°. The aerodynamic performances of those airfoils serve as a database for rotor thrust and torque prediction of the rotor for helicopter forward flight.

The XH-59A rotor thrust, torque and power, under 0.1~0.4 advance ratio in steady forward flight will be presented in the final paper.

6. Contact Author Email Address

Postgraduate, School of Aeronautics: Zsz-1997@mail.nwpu.edu.cn

Associate Professor, School of Aeronautics: xuzhao@nwpu.edu.cn

Postgraduate, School of Aeronautics: 1479481621@qq.com

Postgraduate, School of Aeronautics: kangminghui@mail.nwpu.edu.cn

Senior engineer: lenovo37213618@sina.com

7. Copyright Statement

8. Acknowledgments

This work was supported by the Aeronautical Science Foundation of China 20175753030 and Foundation of National Key Laboratory 20210301-3.

References

[1] Y. Ai. Numerical simulation research on the flow field of the aircraft at a large angle of attack [D]. Nanjing University of Science and Technology, 2015.

[2] T. Zhou. Research on aerodynamic characteristics of high-speed helicopter rigid rotor with large

advance ratio[D]. Nanjing University of Aeronautics and Astronautics, 2018.

[3] W-H Kong, R-L Chen. Effect of Reverse Flow Region on Characteristics of Compound High Speed Helicopter Rotor[J]. Acta Aeronautica Sinica, 2011, 32(02): 223-230.

[4] Paglino V-M, Beno E-A. Full-scale wind-tunnel investigation of the advancing blade concept rotor system [R]. Technical report, USAAMRDL TR 71-25, 1971.

[5] M-C Yuan, Y-F Yang, Y-F Lin, CFD Analysis on Aerodynamic Characteristics of Blade Profiles in Reverse Flow Region of High Speed Helicopter Rotor[J]. Helicopter Technology, 2015(01):1-5+12.

[6] Tapan K. Sengupta, Ashish Bhole, N.A. Sreejith. Direct numerical simulation of 2D transonic flows around airfoils[J]. Computers and Fluids, 2013, 88:19-37.